



An Analysis of the Macroscopic Tensile Behavior of a Nonlinear Nylon Reinforced Elastomeric Composite System Using MAC/GMC

Mahmoud Assaad
The Goodyear Tire & Rubber Company, Akron, Ohio

Steven M. Arnold
Glenn Research Center, Cleveland, Ohio

National Aeronautics and
Space Administration

Glenn Research Center

Acknowledgments

The authors would like to express their thanks to the following two researchers from the Goodyear Tire & Rubber Company: Cheng Shaw of the Polymer Physics Research department for generating the experimental data for single ply laminae, and to Yao-Min Huang of Reinforced Composites Science department for providing the experimental data for the multi ply laminates.

Trade names or manufacturers' names are used in this report for identification only. This usage does not constitute an official endorsement, either expressed or implied, by the National Aeronautics and Space Administration.

Available from

NASA Center for Aerospace Information
7121 Standard Drive
Hanover, MD 21076
Price Code: A03

National Technical Information Service
5285 Port Royal Road
Springfield, VA 22100
Price Code: A03

An Analysis of the Macroscopic Tensile Behavior of a Nonlinear Nylon Reinforced Elastomeric Composite System Using MAC/GMC

by

Mahmoud Assaad

The Goodyear Tire & Rubber Company
Akron, Ohio

and

Steven M. Arnold

NASA Lewis Research Center
Cleveland, Ohio 44135

Abstract

A special class of composite laminates composed of soft rubbery matrices and stiff reinforcements made of steel wires or synthetic fibers is examined, where each constituent behaves in a nonlinear fashion even in the small strain domain. Composite laminates made of plies stacked at alternating small orientation angles with respect to the applied axial strain are primarily dominated by the nonlinear behavior of the reinforcing fibers. However; composites with large ply orientations or those perpendicular to the loading axis, will approximate the behavior of the matrix phase and respond in even a more complex fashion for arbitrarily stacked plies. The geometric nonlinearity due to small cord rotations during loading was deemed here to have a second order effect and consequently dropped from any consideration. The user subroutine USRMAT within the Micromechanics Analysis Code with the Generalized Method of Cells (**MAC/GMC**), was utilized to introduce the constituent material nonlinear behavior. Stress-strain behavior at the macro level was experimentally generated for single and multi ply composites comprised of continuous Nylon-66 reinforcements embedded in a carbon black loaded rubbery matrix. Comparisons between the predicted macro composite behavior and experimental results are excellent when material nonlinearity is included in the analysis. In this paper, a brief review of **GMC** is provided, along with a description of the nonlinear behavior of the constituents and associated constituent constitutive relations, and the improved macro (or composite) behavior predictions are documented and illustrated.

1.0 Introduction

In flexible or soft composites, the high modulus, low elongation cords carry most of the load, and the low modulus, high elongation rubber matrix preserves the integrity of the composites and transfers the load. The primary objective of this type of composite is to sustain large deformation and fatigue loading while providing high load carrying capacity.

The classical approach of establishing the constitutive law for such composites is based on the traditional and well developed anisotropic theory of stiff laminates for small linear elastic deformations. Many reviews have demonstrated the suitability of this approach in predicting the elastic properties and the overall behavior of these composites under different types of deformation fields¹. In this paper, the effort is focused on capturing the material nonlinearity by an alternative micromechanical modeling of composites approach; that is, one which utilizes the mechanical and physical characteristics of both constituents to describe the macro behavior of the composite.

Recently, the Method of Cells (**MOC**)^{2,3,4} and its extension the Generalized Method of Cells (**GMC**)^{5,6,7} have emerged as an efficient micromechanical approach that can predict the micro and macro performance of composites. The method accounts in an explicit fashion for the geometric and mechanical attributes of the constituents, a feature that distinguishes **GMC** from all other averaging schemes (micromechanical models). These capabilities are captured in software packages such as the Micromechanics Analysis Code (**MAC/GMC**)⁸, and the First -Order Nonlinear Elasticity (**FONE**)² code. These codes are structured in a modular fashion that allow a user to implement additional constitutive models through a user defined subroutine. It is this additional feature in **MAC/GMC** that the present work capitalizes upon through the implementation of a nonlinear elastic constitutive model for each constituent.

NASA Glenn Research Center has developed a user-friendly software package (**MAC/GMC**) based on the generalized method of cells (**GMC**) and coupled it with classical lamination theory. The basic formulation of this micromechanical model expresses in explicit fashion the influence of fiber (cord) diameter, inter fiber distance, intra ply gauge, and the constituents' mechanical properties on the global (macro) and local (micro) behavior of the composites. The code was tested against diverse composite configurations and results were compared to available experimental results with favorable agreement^{7,9}. More recently, it was found that the linear elastic model included in **MAC/GMC** was adequate in performing analysis of elastomeric composites reinforced with steel wires with the applied load in the wire direction. However, for synthetic cords such as nylon, polyester, and rayon, and for cases where the load is orthogonal or oriented at a large angle with respect to the direction of the reinforcing cords, the predicted macro results using linear elastic assumptions deviated noticeably from the experimental data. This is due primarily to the nonlinear behavior of the reinforcing cords and the rubbery matrix. To circumvent this discrepancy, a nonlinear elastic material model for the reinforcing cord and two separate constitutive laws for the rubber matrix were formulated by accounting for incompressibility and the observed softening behavior; all nonlinear models were implemented into **MAC/GMC** via its user defined subroutine **USRMAT**.

The present paper begins with a brief mathematical description of **GMC** in section 2. In section 3 the relevant constituent constitutive laws are described. Finally, in section 4, using both linear and nonlinear constitutive models, the numerical predictions obtained from **MAC/GMC** and their corroboration with experimental data are documented.

2.0 Generalized Method of Cells (GMC)

GMC can predict the elastic and inelastic thermomechanical response of both continuous and discontinuous multiphased composite materials with an arbitrary internal microstructure and reinforcement shape. It is a continuum-based micromechanics model that provides closed-form expressions for the macroscopic composite response in terms of the properties, size, shape, distribution, and response of the individual constituents or phases that make up the material. These constituent materials can be represented using **any** elastic and/or viscoplastic deformation and life (e.g., continuum damage mechanics fatigue model) model. The periodic nature of composites typically allows one to identify a repeating unit cell that can be used as a building block to construct the entire composite. The properties of this unit cell are thus representative of the properties of the entire assemblage. In the original **MOC** the unit cell consisted of a single fiber (cord) subcell surrounded by three matrix subcells, however in **GMC** this has been generalized such that the unit cell is subdivided into an arbitrary number of subcell phases. In Fig. 1 a periodic assemblage and repeating unit cell are illustrated, from which the approximate description of the composite is developed.

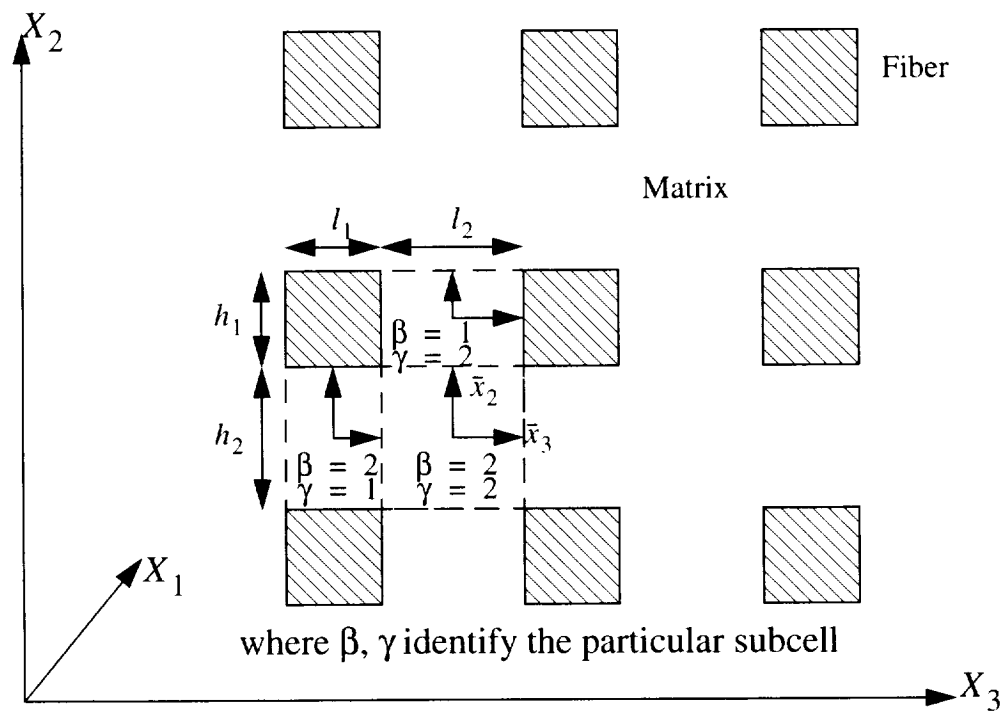


Figure 1. RVE for a continuous fiber reinforced composite.

The basic approach has been presented elsewhere by Aboudi and co-workers^(4 - 8); here only the basic steps required are briefly outlined and have been simplified to address linear elastic material behavior and mechanical loading only. The relations derived are for unidirectional fiber reinforced materials with pseudo square fibers extending in the x_1 direction and arranged in a doubly periodic array in the x_2 and x_3 directions (see Fig. 1). Given the repeating unit cell, identified in Fig. 1 by dotted lines, and the four new local coordinate systems $(\bar{x}_2^{(\beta)}, \bar{x}_3^{(\gamma)})$ introduced at the center of each β, γ subcell, one begins by constructing a first order theory in which the displacements are expanded linearly in terms of the distances from the center each subcell. That is,

$$u_i^{(\beta\gamma)} = w_i^{(\beta\gamma)} + \bar{x}_2^{(\beta)} \varphi_i^{(\beta\gamma)} + \bar{x}_3^{(\gamma)} \psi_i^{(\beta\gamma)} \quad i = 1, 2, 3 \quad (1)$$

where $w_i^{(\beta\gamma)}$ are the displacement components at the center of each subcell, and, $\varphi_i^{(\beta\gamma)}$ and $\psi_i^{(\beta\gamma)}$ characterize the linear dependence of the displacements on the local coordinates, (see Fig. 1).

The components of the small strain tensor are given as follows:

$$\varepsilon_{ij}^{(\beta\gamma)} = \frac{1}{2} [\partial_i u_j^{(\beta\gamma)} + \partial_j u_i^{(\beta\gamma)}] \quad i, j = 1, 2, 3 \quad (2)$$

$$\text{where } \partial_1 = \frac{\partial}{\partial x_1}, \quad \partial_2 = \frac{\partial}{\partial \bar{x}_2^{(\beta)}} \text{ and } \partial_3 = \frac{\partial}{\partial \bar{x}_3^{(\gamma)}}$$

Next the classical linear elastic constitutive relationship is assumed for both fiber and matrix so that the corresponding stiffness matrix is strain independent, that is,

$$\sigma^{(\beta\gamma)} = C^{(\beta\gamma)} \varepsilon^{(\beta\gamma)} \quad (3)$$

where $C^{(\beta\gamma)}$ is the elastic stiffness matrix expressed in terms of the engineering constants of the subcell.

The average stresses in the composite, $\bar{\sigma}_{ij}$, are determined from the average stresses, $\bar{\sigma}_{ij}^{(\beta\gamma)}$, in the subcells, i.e.;

$$\bar{\sigma}_{ij} = \frac{1}{V} \sum_{\beta, \gamma = 1}^2 v_{\beta\gamma} \bar{\sigma}_{ij}^{(\beta\gamma)} \quad (4)$$

where $v_{\beta\gamma} = h_\beta h_\gamma$, $V = (h_1 + h_2)^2$, which is the area of the repeating unit cell, and

$$\bar{\sigma}_{ij}^{(\beta\gamma)} = \frac{1}{v_{\beta\gamma}} \int_{-h_\beta/2}^{h_\beta/2} \int_{-h_\gamma/2}^{h_\gamma/2} \sigma_{ij}^{(\beta\gamma)} d\bar{x}_2^{(\beta)} d\bar{x}_3^{(\gamma)} \quad (5)$$

To establish the composite constitutive relations, the continuity of tractions and displacements are imposed at the boundaries, in an average sense, between the constituents. The continuity of the displacements at the interfaces of each subcell will provide relationships between the average stresses and average strains in the composites and the microvariables in the subcells of the representative cell. The conditions for the continuity of tractions provide the average normal stresses after lengthy mathematical manipulations. For the sake of completeness and yet without the loss of simplicity, only a brief examination of the governing equations is provided.

The condition of continuous normal and tangential displacements at the interfaces of the RVE are imposed on an average basis between subcells (1γ) and (2γ) , for example:

$$\int_{-\frac{h_\gamma}{2}}^{\frac{h_\gamma}{2}} u_i^{(1\gamma)} \Big|_{\bar{x}_2^{(1)} = -\frac{h_1}{2}} d\bar{x}_3^{(\gamma)} = \int_{-\frac{h_\gamma}{2}}^{\frac{h_\gamma}{2}} u_i^{(2\gamma)} \Big|_{\bar{x}_2^{(2)} = \frac{h_2}{2}} d\bar{x}_3^{(\gamma)} \quad (6)$$

From these conditions, the average strain in the subcells can be obtained. The average strains in the composite are given by:

$$\bar{\epsilon}_{ij} = \frac{1}{V} \sum_{\beta, \gamma=1}^2 v_{\beta\gamma} \bar{\epsilon}_{ij}^{(\beta\gamma)} \quad (7)$$

This equation establishes relationships between the average stresses and microvariables in the subcells of the RVE.

The condition of equal average normal, axial and transverse stresses across the interfaces provides needed algebraic equations to determine all unknown microvariable parameters. Eventually, the following composite constitutive relations are established in the form:

$$\bar{\sigma} = B\bar{\epsilon} \quad (8)$$

where $\bar{\sigma}$ are the average macro composite stresses, $\bar{\epsilon}$ are the uniform applied macro composite strains, and B is the effective elastic stiffness tensor defined in terms of the concentration matrix $A^{(\beta\gamma)}$ of the micro subcell, and the elastic stiffness tensor $C^{(\beta\gamma)}$ of each subcell:

$$B = \frac{1}{h_1 h_2} \sum_{\beta=1}^2 \sum_{\gamma=1}^2 h_{\beta} h_{\gamma} C^{(\beta\gamma)} A^{(\beta\gamma)} \quad (9)$$

This was a brief summary of the equations that form the basis of the micro-to-macromechanics analysis which describe the behavior of a heterogeneous media. A more generalized version of this method consisting of, discontinuous as well as continuous fiber reinforcement subcells, inelastic material response, and thermomechanical load histories, has been fully developed and implemented within **MAC/GMC**⁸. **MAC/GMC** has uniquely enhanced the basic capabilities of **GMC** in numerous ways. The one which will be exploited in this work, is the fact that a variety of constituent constitutive models can be accessed via a library of constituent constitutive models or conveniently implemented through a user definable subroutine. The following is a demonstration of how one can modify the linear elastic model provided in **MAC/GMC** into a more elaborate nonlinear elastic model that can better describe the mechanical response of the constituents.

3.0 Characterization of Nonlinear Elastic Constitutive Laws

Currently **MAC/GMC** provides, in addition to three viscoplastic models (Bodner-Partom, Robinson Viscoplastic, and Generalized Viscoplasticity with Potential Structure) and one linear transversely isotropic model, a user-definable constitutive model that can be applied to either (or both) fiber and matrix constituents in a composite. Subsequently, whenever the use of a linear (strain-independent) model is described, this implies use of the built in transversely isotropic model supplied within **MAC/GMC**, yet specialized to its isotropic equivalency. To deduce the fundamental constants such as the axial and shear moduli, a least square approximation of the experimental data for each constituent was employed; wherein the modulus of elasticity of the rubber compound was determined to be 1.87 ksi and that of the reinforcing cord to be 282.36 ksi. Consequently the strength of anisotropy is approximately 151. The specification and characterization of the nonlinear (strain-dependent) reversible models for both cord and rubber matrix are described below.

3.1 Fiber Reinforcement

The composite samples used for this study, were manufactured with multi filament Nylon 66 cords twisted in 3 strands with a 5x5 twist per inch (each strand is twisted with 5 twists per inch in a direction that gives it an S shape appearance, then the cord is formed by twisting all 3 strands with 5 twists per inch in an opposite direction that gives it a Z shape appearance) and a matrix made of a moderately carbon black loaded natural rubber. The axial behavior of the reinforcing cord was determined from the experimental macroscopic stress-strain response under strain control with a strain rate of 12 in/in/min; see Fig. 2.

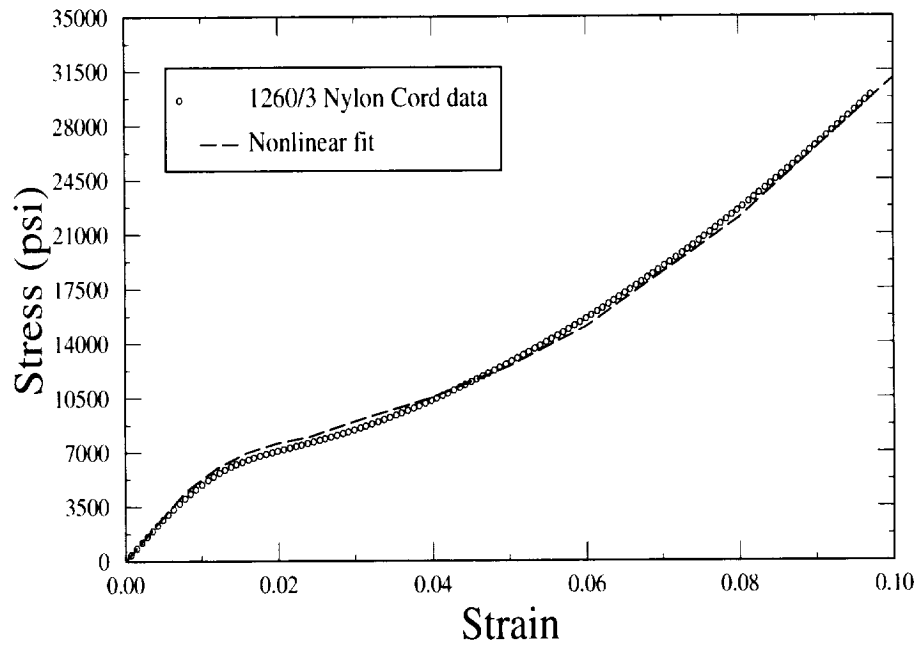


Figure 2. Nonlinear behavior of a 1260/3 Nylon cord

In the absence of an explicit constitutive law for the nylon cord, a phenomenological nonlinear model was utilized; wherein the cord was idealized as a structure in and of itself. The nonlinearity was introduced by considering the resulting discretized macroscale cord modulus to be strain dependent as shown in Table 1. The corresponding nonlinear fit is also shown in Fig. 2.

TABLE 1. Cord Moduli as function of the strain level

Strain level ϵ	Modulus-Msi
0.0 - 0.008	$- 17.25\epsilon + 0.700$
0.008 - 0.012	$- 15.50\epsilon + 0.686$
0.012 - 0.016	$- 15.75\epsilon + 0.689$
0.016 - 0.02	$- 14.25\epsilon + 0.665$
0.02 - 0.024	$- 11.75\epsilon + 0.615$
0.024 - 0.03	$- 5.50\epsilon + 0.465$

TABLE 1. Cord Moduli as function of the strain level

Strain level ϵ	Modulus-Msi
0.03 - 0.04	$- 3.70\epsilon + 0.411$
0.04 - 0.05	$- 1.30\epsilon + 0.315$
0.05 - 0.06	$0.10\epsilon + 0.245$
0.06 - 0.08	$1.20\epsilon + 0.179$
0.08 - 0.10	$1.75\epsilon + 0.135$

Note, this is only a partial description of how the cord modulus changes over the range of the applied strain. One can extend the description over the expected domain of application.

3.2 Rubber Matrix

Rubber compounds are widely used as the continuous phase in elastomeric composites. Although, their behavior is constrained by the presence of the reinforcing fibers (cords), there are instances where the overall composite behavior is predominantly dictated by that of the rubber, e.g., when the composite is loaded transverse to the fiber direction. Essentially, these materials can undergo large deformations while remaining elastic. The continuum mechanics theory used to model such behavior is called hyperelasticity. This theory can be formulated in terms of principal invariants and principal stretches with an additional parameter to treat the incompressibility of the material. The Mooney-Rivlin and Ogden models⁽¹⁰⁾ are best suited for very large deformations. Alternatively, in the small deformation regime, the classical isotropic linear elasticity model, expressed with a bulk modulus and a shear modulus as a function of strain, is a very convenient approach to implement in **MAC/GMC**.

3.2.1 Classical Elasticity Extended

Isothermal linear elasticity assumes a linear relationship between the Cauchy stress and the total infinitesimal strain. But, with proper modification, the nonlinear behavior of the rubber is captured by establishing the dependency of its elastic stiffness tensor on the level of strain magnitudes. In addition, the incompressibility of the rubber was captured in the hydrostatic component of the total stress by assigning a value close to 0.5 for the Poisson's ratio. The following traditional stress decomposition into two components is utilized:

$$\sigma_{ij} = -p\delta_{ij} + S_{ij} \quad (10)$$

where p is the hydrostatic stress component and is related to the volumetric strain ϵ_{kk} and the bulk modulus, K , by the following relations:

$$p = K\varepsilon_{kk}, \text{ with } K = \frac{E}{3(1-\nu)} \quad (11)$$

where E represents the Young's modulus and ν the Poisson's ratio of the given material.

The deviatoric stress, S_{ij} , components are related to the associated deviatoric strain components e_{ij} and the shear modulus G as follows:

$$S_{ij} = Ge_{ij} \quad (12)$$

wherein, the deviatoric strains are related to the total strains, ε_{ij} , and the volumetric strains according to the following relationship:

$$e_{ij} = \varepsilon_{ij} - \varepsilon_{kk}\delta_{ij} \quad (13)$$

For computational purposes, a more useful form of the constitutive law can be presented in tensorial form as follows:

$$\sigma_{ij} = C_{ijkl}\varepsilon_{kl} \quad (14)$$

where the elastic stiffness tensor C_{ijkl} is presented in matrix form as follows:

$$[C] = \begin{bmatrix} K + \frac{4}{3}G & K - \frac{2}{3}G & K - \frac{2}{3}G & 0 & 0 & 0 \\ K - \frac{2}{3}G & K + \frac{4}{3}G & K - \frac{2}{3}G & 0 & 0 & 0 \\ K - \frac{2}{3}G & K - \frac{2}{3}G & K + \frac{4}{3}G & 0 & 0 & 0 \\ 0 & 0 & 0 & G & 0 & 0 \\ 0 & 0 & 0 & 0 & G & 0 \\ 0 & 0 & 0 & 0 & 0 & G \end{bmatrix} \quad (15)$$

The nonlinearity of the rubbery material was added to this elastic Hookean constitutive law by expressing the shear modulus as a function of the applied strain magnitude, so as to account for the network decay and compound breakdown. The strain dependency of the modulus of the carbon black filled rubber was first reported by Payne¹¹ but it was also theoretically approached, by Kraus¹². Herein, the elastic modulus G is described using an Arrhenius type relationship characterizing its exponential decay,

$$G = G_0 e^{(-\alpha \gamma)} \quad (16)$$

where G_0 is the initial modulus in the absence of any previous history, γ is the applied strain amplitude, and α is a phenomenological constant that describes the dependency of the modulus of the material on the strain softening and the irreversible breakdown under static strain. G_0 and α are material parameters that can be determined experimentally.

To generalize the above uniaxial dependency of the shear modulus to that of a multiaxial deformation field, eq. (16) can be rewritten as:

$$G = G_0 e^{(-\alpha \sqrt{I_1 - 3})} \quad (17)$$

where $I_1 = (\lambda_1 + \lambda_2 + \lambda_3)$. Now given an incompressible or nearly incompressible body ($I_3 = \lambda_1 \lambda_2 \lambda_3 = 1$) under pure shear deformation (i.e., $\lambda_1 = \lambda^2, \lambda_2 = 1, \lambda_3 = \frac{1}{\lambda^2}$) it can be shown that I_1 becomes,

$$I_1 = \lambda^2 + 1 + \frac{1}{\lambda^2} \quad (18)$$

Also, given the fact that the strain in the torsional deformation mode considered in the analysis can be approximated in terms of the stretch ratio λ as,

$$\gamma \approx \tan \gamma = \lambda - \frac{1}{\lambda} \quad (19)$$

such that upon squaring the stretch, i.e., $\gamma^2 = I_1 - 3$, one can clearly see that eq. (17) reduces to the uniaxial expression given in eq. (16).

In order to characterize eq. (16), a laboratory testing procedure was implemented using systematic sweeps of increasing strain amplitude performed on parallel plate specimen subjected to torsional shear. A characterization temperature of 25°C and a frequency of 1 Hz were selected on the Rheometrics System IV to achieve the best reproducibility over the entire strain range. The correlation delay was set to 10 seconds, so that a 3 to 5 cycle break-in would occur prior to the response measurement. From the 10 experiments, 275 stress strain data pairs were obtained, from which a subset of data representing shear modulus verses strain was established (see Figure 3). Such a set of data is usually sufficient to perform a non-linear least squares regression, leading to the determination of the parameters G_0 and α . A numerical method based on the Marquardt-Levenberg approach

was used to perform non-linear regression to obtain the two parameters G_0 and α . For a typical cured rubber compound at room temperature these two constants are $G_0 = 5.237$ ksi, and $\alpha = 14.713$.

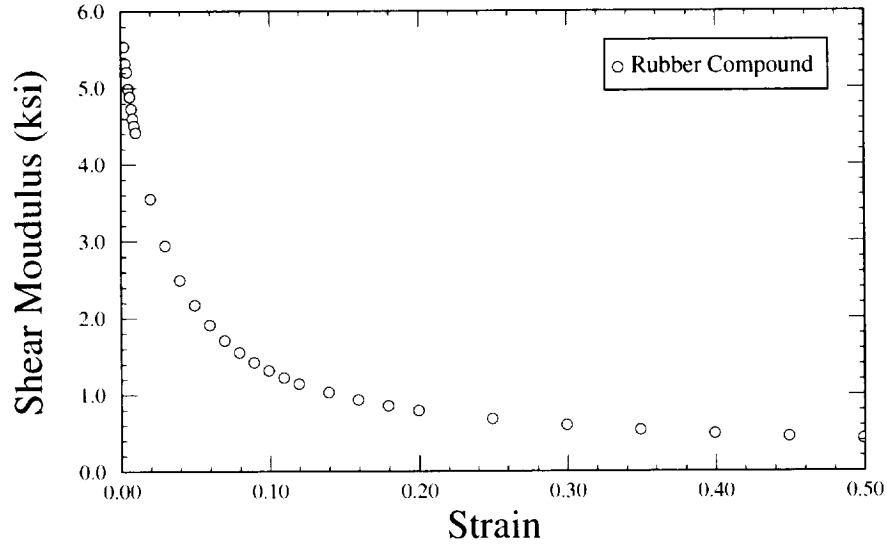


Figure 3. Shear Moduli as a function of strain level

3.2.2 Mooney-Rivlin

To demonstrate the versatility of the software package **MAC/GMC**, and to provide an alternative way to implement a given constitutive law, a strain energy based model was introduced and compared against the previous model. The polynomial Mooney-Rivlin strain energy function was chosen to account for the material nonlinearity and incompressibility of the rubbery matrix as follows:

$$W = C_1(I_1 - 3) + C_2(I_2 - 3) + K(I_3 - 3) \quad (20)$$

where C_1 , C_2 are two material constants, K represents the material incompressibility, and I_1, I_2, I_3 are the three strain invariants defined as follows:

$$I_1 = tr(c) = c_{ii}$$

$$I_2 = \frac{1}{2}(tr^2(c) - tr(c^2)) = \frac{1}{2}(c_{kk}c_{kk} - c_{ik}c_{kj})$$

$$I_3 = \det|c_{ij}| \quad (21)$$

where c is the Lagrangian strain tensor defined in terms of the deformation tensors ($c = F^T F$) and expressed as function of the strain components as follows:

$$\epsilon_{ij} = \frac{c_{ij} - \delta_{ij}}{2} \quad (22)$$

The associated Second Piola-Kirchhoff stress tensor (S_{ij}) is obtained by differentiating with respect to the strain using the chain rule as follows:

$$S_{ij} = 2 \frac{\partial W}{\partial c_{ij}} = 2 \left(\frac{\partial W}{\partial I_1} \frac{\partial I_1}{\partial c_{ij}} + \frac{\partial W}{\partial I_2} \frac{\partial I_2}{\partial c_{ij}} + \frac{\partial W}{\partial I_3} \frac{\partial I_3}{\partial c_{ij}} \right) \quad (23)$$

by substituting for the derivatives of the strain invariants and simplifying the following expression is obtained:

$$S_{ij} = 2 \left(c_1 \delta_{ij} + c_2 (I_1 \delta_{ij} - c_{ij}) + \frac{K}{\det|c_{ij}|} (c^{-1})_{ij} \right) \quad (24)$$

Two hypothetical cases of an RVE containing four subcells, with properties taken to be those of the matrix, were analyzed with the two types of material models described above. The same strain-softening function for the matrix material was implemented into the **USRMAT** formulation. The macro stress-strain calculated by **MAC/GMC** is plotted in Fig. 4 and illustrates the excellent agreement between both nonlinear models and the experimental data.

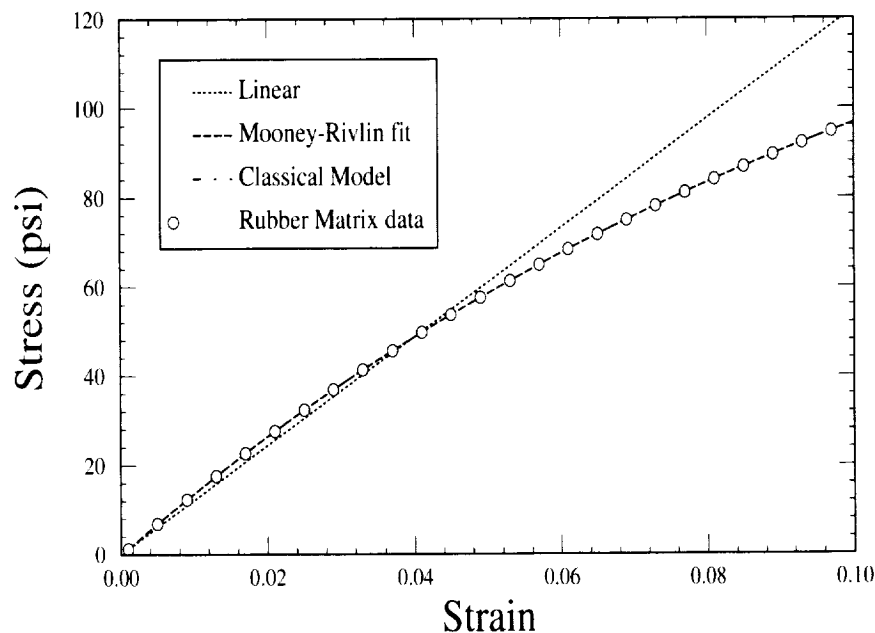


Figure 4. Comparison between the classical and strain energy material models

4.0 Results

By incorporating in **MAC/GMC** either type of nonlinear constitutive law for the rubber behavior (including softening and incompressibility features) in addition to the strain dependency of the cord modulus the most accurate composite response is expected. To demonstrate this, an experimental program was conducted for single and multi-ply laminates. Comparison of the experimental results with numerical predictions of the composite behavior, based on the previously discussed constituent fiber/matrix constitutive laws, is discussed below. Note, all macro calculations represent true predictions as only constituent cord and matrix behavior were correlated with experimental data and a strong bond was assumed to be present between cord and matrix phases.

4.1 Unidirectional Composite

A set of single ply unidirectional specimens with the dimensions L 12" x W 1" x T 0.035" were built with each having approximately a 24 percent fiber volume ratio and a preferred direction of either [0], [30], [45] or [90] degrees. A gray square was drawn on the surface of each sample in the middle region where strains were measured in the principal directions. Displacements and induced axial and lateral forces were recorded by a video camera and a load cell respectively. The load-displacement data from the composite samples were converted into stress-strain data for a direct comparison with the output generated by **MAC/GMC**. A **MAC/GMC** input file⁸ is listed in **Appendix A** for the case

where the mechanical properties of the reinforcing cord were assumed linear, i.e., to be constant and independent of strain magnitude.

The 12 inch sample length was adopted after conducting an aspect ratio study⁽¹³⁾ in which little to no change in the uniformity of the strain field at the center of the sample was observed for specimens of this length and longer. In addition, the various correction factors were examined for the elastic properties discussed in the literature⁽¹⁴⁾ for off-axis laminae testing. It was determined that the specimen aspect ratio of length and width utilized was sufficient so that no correction associated with axial-shear coupling was required.

Furthermore, a study was conducted to investigate the influence of the assumption of periodicity which is at the core of the MOC and GMC formulation. Consequently, composite laminates with the same cord volume fraction ($V=0.247$) were cured into one, two and four [0] ply laminates. The samples were cut into similar dimensions as discussed above and tested under the same loading conditions. The macro stress-strain responses were recorded and compared with little to no difference being observed; due to the large modulus mismatch between cord and matrix and the fact that the response of the lamina is dominated by the cord.

The samples were uniaxially stretched with an Instron Model 1122. The lateral and longitudinal strains were measured by an image processing system which include a CCD video camera, a NuVision image processing unit and software developed by Perceptics Corporation. An optical target was drawn at the center of the samples with a silver pen as shown in Fig. 5. The target was deformed into a lozenge shape when the specimen was stretched. The maximum and minimum dimensions of the lozenge, which can be converted into longitudinal and lateral strains, were obtained during the measurement. Each test was repeated 3 times with a new specimen, the repeatability was reasonably good, and the average values were reported.

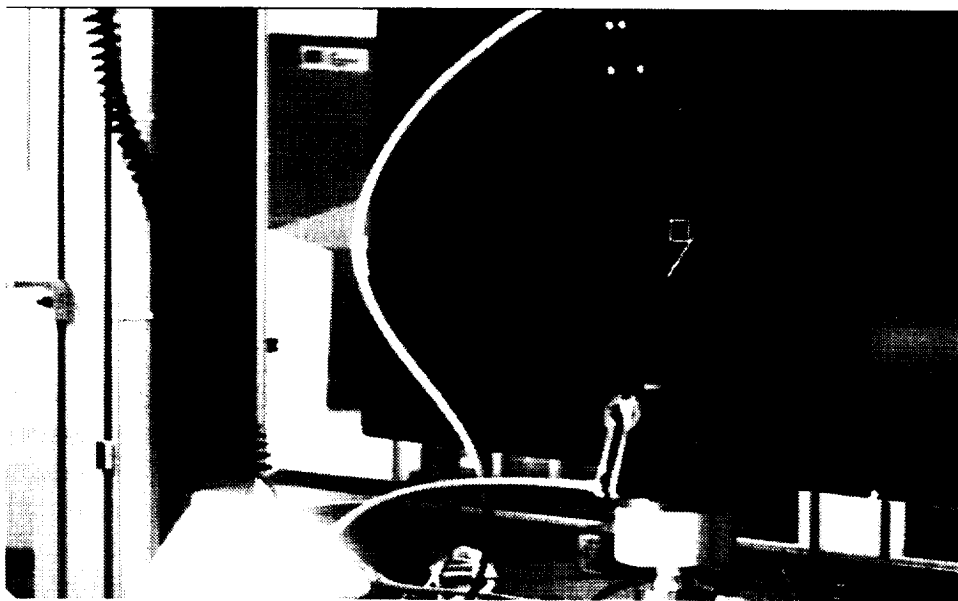


Figure 5 Test fixture

Comparison between the experimental and numerically predicted composite tensile response for all four cord orientations, i.e., [0], [90], [30] and [45] are shown in Figs. 6-8. Two predictions are shown per orientation, one employing a linear constituent constitutive model and the other a nonlinear (strain-dependent) for both cord and matrix phase. As one might expect, the importance of including nonlinearity in a given phase (cord and/or matrix) is highly dependent upon the ply orientation. Considering, the [0] degree laminate, as shown in Fig. 6, it is clear that in the small strain domain between 0.0 and 0.02, the maximum discrepancy of the linear model is on the order of 4.0%, and increases to a maximum of 12.0% for the larger strain magnitude of 0.1. This discrepancy, however, is significantly reduced by accounting for the nonlinearity of the cord behavior as in this case the composite response is dominated by that of the cord. Alternatively, for the case when the applied strain direction is perpendicular (i.e., transverse) to the cord direction the rubbery matrix phase now becomes the dominate constituent influencing the composite response, see Fig. 7. Examining Fig. 7, it is clear that utilizing either a classical or Mooney-Rivlin nonlinear model (implemented through the user defined material model) for the rubbery matrix provides the most accurate composite tensile prediction. Also, the assumption of a strong fiber/matrix bond, as stipulated in the analysis, is clearly justified since the composite response is stiffer (although only slightly due to the low volume fraction) than that of the matrix alone.

The additional feature related to the rubber incompressibility was not fully explored to the same depth as the softening effect. It is believed that under the extensional deformation mode investigated in this paper, the primary source of nonlinearity is affecting the shear modulus of elasticity more than the bulk modulus. Therefore, the results reported in Fig. 7 were generated with a Poisson's ratio of 0.49 and a constant bulk modulus of $K = 10.475$ ksi.

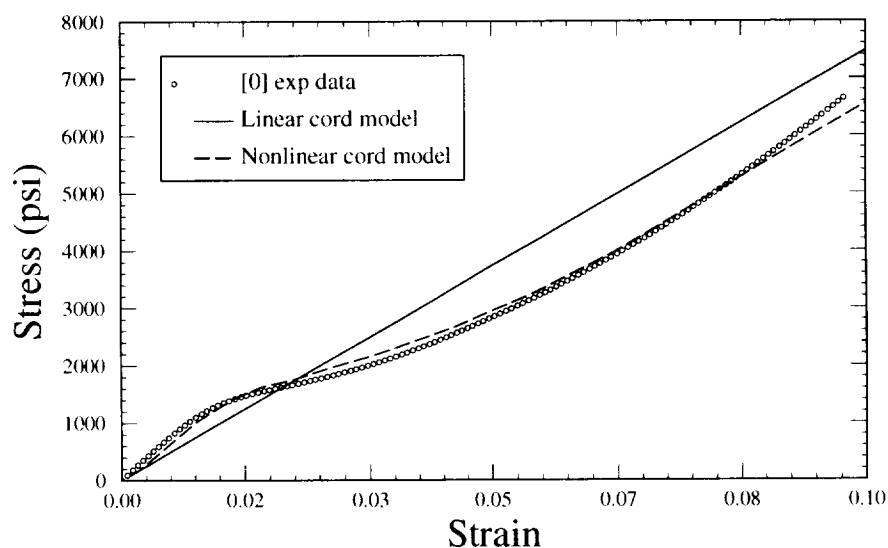


Figure 6. Stress-strain comparison for [0] degree ply.

Similar improvements in the accuracy (when using a nonlinear material model for the constituents) of the predicted composite behavior as compared to that measured, are observed for the two off-axis (i.e., [30] and [45]) tests with respect to applied strain direction, shown in Fig. 8. In the case of the [30] laminate, the linear cord and matrix model will start deviating from the actual data at approximately 0.04 strain, whereas when the nonlinear cord and matrix model are utilized the range of accuracy is increased up to approximately 0.08 strain with the discrepancy between linear and nonlinear predictions verses observed data being a factor of two at 0.12 strain, where the nonlinear model under-predicts the experimental data by approximately 12% and the linear over-predicts by approximately 26%. A similar trend (although not shown in Fig. 8) was noted for the other angles with the discrepancy between linear and nonlinear model predictions versus experimental data for the [90] ply orientation being as much as a factor of six.

Such lack of accuracy at large strain values is expected, since for large orientation angles the amount of cord reorientation becomes significant and the overall response is dominated not only by the nonlinear behavior of the cord and matrix but also the geometric nonlinearity and its effects on the stiffness of the composites.

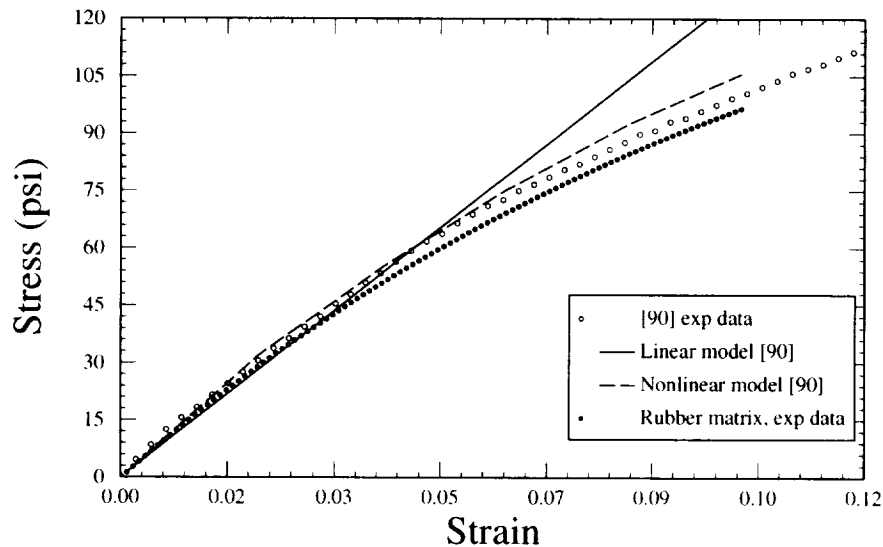


Figure 7. Stress-strain comparison for [90] degree ply.

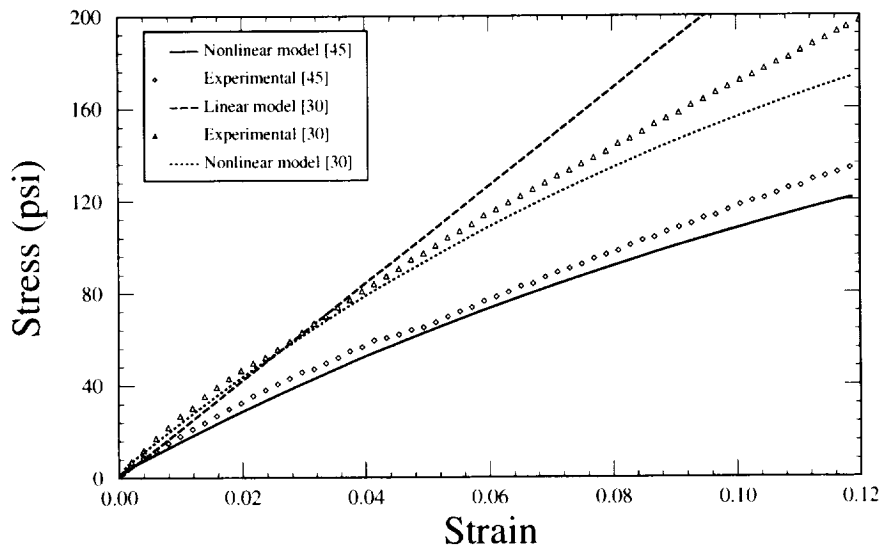


Figure 8. Stress-strain comparison for off-axis orientations.

Since lateral as well as longitudinal strains were recorded, a comparison between the measured and predicted effective (composite) Poisson's ratio can be made and is shown in Figs. 9 and 10. Predictions were made using both the generalized nonlinear classical elasticity and the Mooney-Rivlin constitutive model for the matrix, described in section 3.2. Clearly, the predictive ability of **MAC/GMC** is very good for all angles of orientation, with a maximum deviation from experimental results of approximately 5 percent. Furthermore, although both cord and matrix constituent properties possess differing degrees of strain dependent nonlinearities; only in the case of [0] and [90] laminae is the effective Poisson's ratio a function of applied strain when using the classical elasticity model. Also, Figs. 9 and 10 demonstrate the fact that only when one examines multiple stress or strain components (here the e_{22} and e_{11} are represented by the effective Poisson's ratio) can a distinction be made between multiaxial representations. For example, in Figs. 9 and 10 we see that the classical elasticity generalization appears to represent the experimental data better than does the Mooney-Rivlin approach discussed in section 3.2.2, as employing the Mooney-Rivlin constitutive model produces a strain dependent effective Poisson's ratio for all ply orientation angles. This is in contrast to the observed experimental behavior.

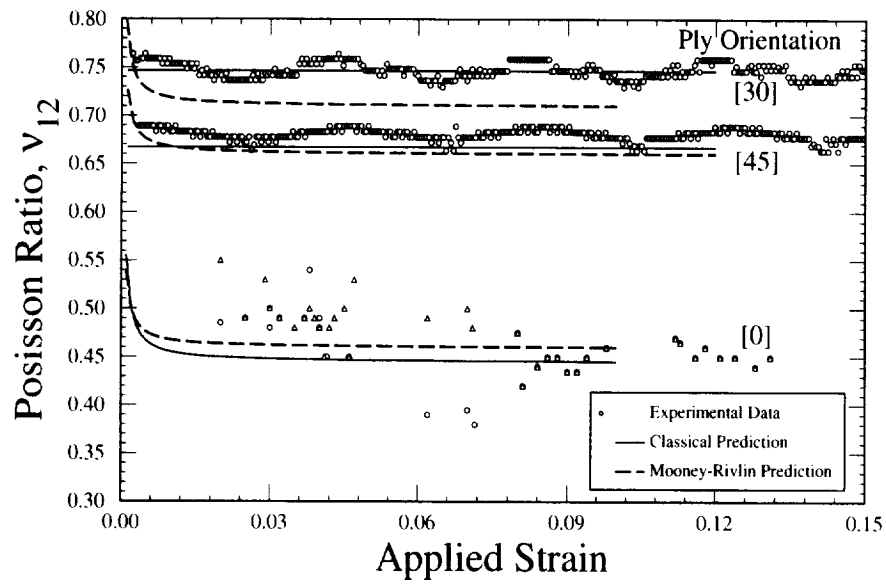


Figure 9 Comparison of predicted and measured effective Poisson's ratio for [0], [30] and [45] ply orientations.

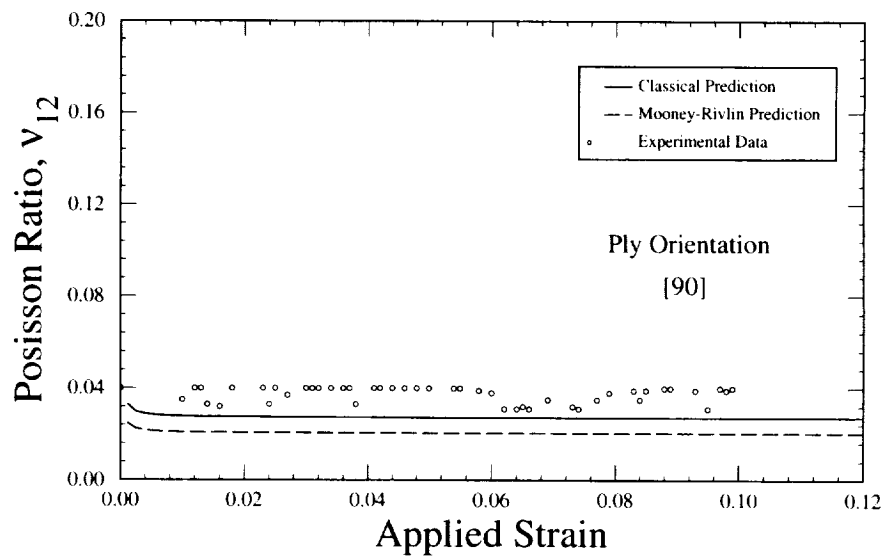


Figure 10 Comparison of predicted and measured effective Poisson's ratio for [90] ply orientation.

4.2 Cross Ply Laminate

A similar analysis was conducted for a cross ply laminate. Here the samples consisted of four plies with the dimensions L 5.5" x W 0.7874" x T 0.22", stacked at 10 degree angles with respect to the applied strain direction in an alternating fashion, i.e., $+[10]$, $-[10]$, $+[10]$, $-[10]$ degree. The samples were first conditioned by subjecting them to 10 loading-unloading cycles to overcome the history imposed on the sample by the mold during the cure cycle, then tested under axial strains. Two example listings of the revised **MAC/GMC** version 2.0 input file are presented in **Appendix B**. The first utilizes the linear elastic model supplied within **MAC/GMC** to represent both the reinforcing cord and matrix. The material properties are supplied by the user as indicated by setting the parameter $IDB=n$. The second illustrates how one would specify the needed parameters to invoke the user defined subroutine.

The experimentally obtained load-extension data was once again converted into stress-strain data so as to conform with the output generated by **MAC/GMC**. As in the unidirectional laminate case, both linear and nonlinear constituent models were applied. As expected, after subjecting the cross ply laminate to the same loading condition as in the unidirectional case, a noticeable improvement in the predictive capability of **MAC/GMC** was realized when nonlinear constituent descriptions were employed, as shown in Fig. 11. The nonlinear cord description being the most important due to the small orientation angle of ± 10 degrees.

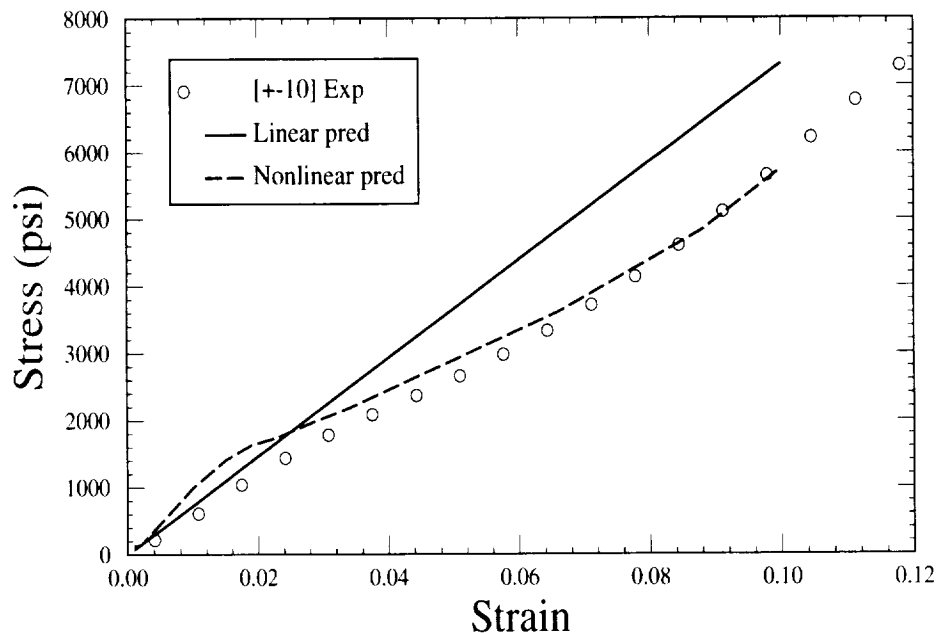


Figure 11. Comparison between experimental data and both models for $[+10]_s$

Close examination of Fig. 11 reveals the superiority of the nonlinear model in predicting the composite behavior in the strain range of 0.05 to 0.10. However, the linear model seems to be more accurate in the strain range below 0.05; a feature left unexplainable due to the lack of sufficient experimental data. Nonetheless, the ability of the nonlinear model to capture the composite behavior was well demonstrated.

5.0 Conclusion

The micromechanical analysis of nylon reinforced elastomeric composites using **MAC/GMC** was greatly enhanced by accounting for the constituent's material nonlinear behavior. The geometric nonlinearity due to small cord rotations during loading was assumed here to have a second order affect and consequently dropped from any further consideration. The user subroutine **USRMAT** within **MAC/GMC**, with analysis capabilities based on the generalized method of cells (GMC), was utilized to introduce the nonlinear constituent material behavior. Stress-strain behavior at the macro level was experimentally generated for single ply unidirectional and multi-ply symmetric laminate, continuously reinforced composites, composed of Nylon-66 embedded in a carbon black loaded rubbery matrix. Comparisons between the predicted macro composite behavior and experimental results, at both lamina and laminate levels were made with the agreement being very good provided the constituent's material nonlinearity was included in the analysis. Also, very good overall agreement with transverse strain measurements via Poisson's ratio were obtained for all ply orientations when utilizing a nonlinear extension of the classical elasticity constitutive model. It is believed that the improvement realized at the macro level will also be observed at the micro level, a concept that will be further investigated in future works.

6.0 Acknowledgment

The authors would like to express their thanks to the following two researchers from the Goodyear Tire & Rubber Company: Cheng Shaw of the Polymer Physics Research department for generating the experimental data for single ply laminae, and to Yao-Min Huang of Reinforced Composites Science department for providing the experimental data for the multi ply laminates.

7.0 References

- 1 R. M. Jones, "Mechanics of Composite Materials", McGraw-Hill Book Company 1975.
- 2 J. B. Aidun, F. L. Addessio, "A Cell Model for Homogenization of Fiber-Reinforced Composites: General Theory and Nonlinear Elasticity Effects". Los Alamos National Laboratory. LA-12904-MS, UC-700, issued: November 1995. J. Comp. Mat. 30, pp. 248 - 280, 1996.

- 3 Addessio, J. B. Aidun, "Analysis of Shock-Induced Damage in Fiber-Reinforced Composites", Los Alamos National Laboratory LA-UR-95-2162.
- 4 Jacob Aboudi, Mechanics of Composite Materials - A Unified Micromechanical Approach. Elsevier Science (Amsterdam 1991).
- 5 Jacob Aboudi, "Micromechanical Analysis of Composites by the Method of Cells-Update". Applied Mechanics Review, vol 49, no 10, part 2, October 1996.
- 6 Jacob Aboudi, "Micromechanical Analysis of Thermo-inelastic Multiphase Short-Fiber Composite". Composites Engineering 5, 839-850.
- 7 S. M. Arnold, M-J Pindera, T. E. Wilt, "Influence of Fiber Architecture of the Inelastic Response of Metal Matrix Composites". International Journal of Plasticity, vol 12, no 4, pp. 507 - 545, 1996.
- 8 T. E. Wilt, S.M. Arnold, "Micromechanics Analysis Code (MAC) ". User Guide version 2.0. NASA Technical Memorandum 107290, August 1996.
- 9 T.E. Wilt, S.M. Arnold, and R. Goldberg, "Micromechanics Analysis Code, MAC Features and Applications," HITEMP REVIEW 1997, Volume II: Advanced Alloys and MMC's, NASA CP 10192, 1997, pp. 30:1-30:13
- 10 L. R. G. Treloar, "The Physics of Rubber Elasticity". Clarendon Press, Oxford 1975.
- 11 A. R. Payne, "Hysteresis in Rubber Vulcanizates". Journal of Polymer Science: Symposium No 48, pp. 169 - 196, 1994
- 12 G. Kraus, "Mechanical Losses in Carbon Black Filled Rubbers". Journal of Applied Polymer Science, Applied Polymer Symposium 39, pp. 75-92, 1984.
- 13 C Shaw, "Poisson's Ratio of Orthotropic Cord-Rubber Composites", Goodyear Internal report, September 30, 1993.
- 14 C. T. Herakovich, Mechanics of Fibrous Composites, John Wiley & Sons, Inc, 1998, see section 6.4.3.2.

Appendix A

Input file for the regular version of **MAC/GMC** using the unidirectional option

Model 0 degree nylon $0.<\epsilon<0.10$

*PRINT

NPL=0 %

*LOAD

LCON=2 LOP=1 LSS=1 %

*MECH

NPTW=2 TI=0.,1. LO=0.,0.10 %

*MODEL

MOD=1 %

*SOLVER

NTF=1 NPTS=2 TIM=0.,1. STP=0.01 %

*FIBER

NFIBS=1

NF=1 MF=6 MAT=6 IDB=n &

EL=0.28236E6,0.282363E5,0.65,0.65,0.1E5,0.,0. %

*MATRIX

NMATX=1

NM=1 MM=6 MAT=A IDB=n &

EL=1.87E3,1.87E3,0.49,0.49,0.690E3,0.,0. %

*MRVE

IDP=11 VF=0.247 RAD=0.0155 R=0.977374 %

*CURVE

NP=1 %

*MACRO

NT=1

NC=1 X=1 Y=7 NAM=nylonregularoutMAC %

*END

A modified input file that utilizes the materials nonlinearity supplied by the user sub-routine USRMAT:

```
Model 0 deg. hyten 0.<e<0.10
*PRINT
  NPL=0 %
*LOAD
  LCON=2 LOP=1 LSS=1 %
*MECH
  NPTW=2 TI=0.,1. LO=0.,0.10 %
*MODEL
  MOD=3 MATSYS=1 NLY=1 THK=0.03583 &
  CON=2 SYS=1 ANG=0. %
*SOLVER
  NTF=1 NPTS=2 TIM=0.,1. STP=0.01 %
*FIBER
  NFIBS=1
  NF=1 MS=1 MF=99 NPE=5 EL=0.28236E6,0.28236E5,0.65,0.65,0.1E5&
  NPV=0 %
*MATRIX
  NMATX=1
  NM=1 MS=1 MM=99 NPE=5 EL=1.87E3,1.87E3,0.49,0.49,0.690E3 &
  NPV=0 %
*MRVE
  IDP=11
  L=1 VF=0.2476 RAD=0.0075 R=0.977374 %
*CURVE
  NP=1 %
*MACRO
  NT=1
  NC=1 X=1 Y=7 NAM=modplyout %
END
```

Appendix B

Input file for the regular version of **MAC/GMC** using the laminate option

Nylon +10/-10/+10/-10 laminate simulation

***PRINT**

NPL=-1 %

***LOAD**

LCON=2 LOP=1 LSS=1 %

***MECH**

NPTW=2 TI=0.,1. LO=0.,0.10 %

***MODEL**

MOD=3 MATSYS=1 NLY=4 THK=0.055,0.055,0.055,0.055 &

CON=2,2,2,2 SYS=1,1,1,1 ANG=+10.,-10.,+10.,-10. %

***SOLVER**

NTF=1 NPTS=2 TIM=0.,1. STP=0.01 %

***FIBER**

NFIBS=1

NF=1 MS=1 MF=6 MAT=6 IDB=n &

EL=0.28236E6,0.28236E5,0.65,0.65,0.1E5,0.,0. %

NPV=0 %

***MATRIX**

NMATX=1

NM=1 MS=1 MM=6 MAT=D IDB=n &

EL=1.87E3,1.87E3,0.49,0.49,0.690E3,0.,0. %

***MRVE**

IDP=11,11,11,11

L=1 VF=0.247 RAD=0.0155 R=0.977374

L=2 VF=0.247 RAD=0.0155 R=0.977374

L=3 VF=0.247 RAD=0.0155 R=0.977374

L=4 VF=0.247 RAD=0.0155 R=0.977374 %

***CURVE**

NP=1 %

***MACRO**

NT=1

NC=1 X=1 Y=7 NAM=nylonlaminatecontrol %

***END**

The modified input file that utilizes the materials nonlinearity supplied by the user subroutine USRMAT:

```
Nylon +10/-10/+10/-10 laminate simulation
*PRINT
  NPL=-1 %
*LOAD
  LCON=2 LOP=1 LSS=1 %
*MECH
  NPTW=2 TI=0.,1. LO=0.,0.10 %
*MODEL
  MOD=3 MATSYS=1 NLY=4 THK=0.055,0.055,0.055,0.055 &
  CON=2,2,2,2 SYS=1,1,1,1 ANG=+10.,-10.,+10.,-10. %
*SOLVER
  NTF=1 NPTS=2 TIM=0.,1. STP=0.01 %
*FIBER
  NFIBS=1
  NF=1 MS=1 MF=99 NPE=5 EL=0.28236E6,0.28236E5,0.65,0.65,0.1E5 &
  NPV=0 %
*MATRIX
  NMATX=1
  NM=1 MS=1 MM=99 NPE=5 EL=1.87E3,1.87E3,0.49,0.49,0.690E3&
  NPV=0 %
*MRVE
  IDP=11,11,11,11
  L=1 VF=0.247 RAD=0.0155 R=0.977374
  L=2 VF=0.247 RAD=0.0155 R=0.977374
  L=3 VF=0.247 RAD=0.0155 R=0.977374
  L=4 VF=0.247 RAD=0.0155 R=0.977374 %
*CURVE
  NP=1 %
*MACRO
  NT=1
  NC=1 X=1 Y=7 NAM=nylonlami
```

REPORT DOCUMENTATION PAGE			Form Approved OMB No. 0704-0188	
Public reporting burden for this collection of information is estimated to average 1 hour per response, including the time for reviewing instructions, searching existing data sources, gathering and maintaining the data needed, and completing and reviewing the collection of information. Send comments regarding this burden estimate or any other aspect of this collection of information, including suggestions for reducing this burden, to Washington Headquarters Services, Directorate for Information Operations and Reports, 1215 Jefferson Davis Highway, Suite 1204, Arlington, VA 22202-4302, and to the Office of Management and Budget, Paperwork Reduction Project (0704-0188), Washington, DC 20503.				
1. AGENCY USE ONLY (Leave blank)		2. REPORT DATE March 1999		3. REPORT TYPE AND DATES COVERED Technical Memorandum
4. TITLE AND SUBTITLE An Analysis of the Macroscopic Tensile Behavior of a Nonlinear Nylon Reinforced Elastomeric Composite System Using MAC/GMC			5. FUNDING NUMBERS WU-505-23-2L-00	
6. AUTHOR(S) Mahmoud Assaad and Steven M. Arnold				
7. PERFORMING ORGANIZATION NAME(S) AND ADDRESS(ES) National Aeronautics and Space Administration John H. Glenn Research Center at Lewis Field Cleveland, Ohio 44135-3191			8. PERFORMING ORGANIZATION REPORT NUMBER E-11620	
9. SPONSORING/MONITORING AGENCY NAME(S) AND ADDRESS(ES) National Aeronautics and Space Administration Washington, DC 20546-0001			10. SPONSORING/MONITORING AGENCY REPORT NUMBER NASA TM-1999-209066	
11. SUPPLEMENTARY NOTES Mahmoud Assaad, The Goodyear Tire & Rubber Company, Akron, Ohio and Steven M. Arnold, NASA Glenn Research Center, Cleveland, Ohio 44135. Responsible person, Steven M. Arnold, organization code 5920, (216) 433-3334.				
12a. DISTRIBUTION/AVAILABILITY STATEMENT Unclassified - Unlimited Subject Categories: 24 and 39 This publication is available from the NASA Center for AeroSpace Information, (301) 621-0390.			12b. DISTRIBUTION CODE	
13. ABSTRACT (Maximum 200 words) A special class of composite laminates composed of soft rubbery matrices and stiff reinforcements made of steel wires or synthetic fibers is examined, where each constituent behaves in a nonlinear fashion even in the small strain domain. Composite laminates made of piles stacked at alternating small orientation angles with respect to the applied axial strain are primarily dominated by the nonlinear behavior of the reinforcing fibers. However, composites with large ply orientations or those perpendicular to the loading axis, will approximate the behavior of the matrix phase and respond in even a more complex fashion for arbitrarily stacked piles. The geometric nonlinearity due to small cord rotations during loading was deemed here to have a second order effect and consequently dropped from any consideration. The user subroutine USRMAT within the Micromechanics Analysis Code with the Generalized Method of Cells (MAC/GMC), was utilized to introduce the constituent material nonlinear behavior. Stress-strain behavior at the macro level was experimentally generated for single and multi ply composites comprised of continuous Nylon-66 reinforcements embedded in a carbon black loaded rubbery matrix. Comparisons between the predicted macro composite behavior and experimental results are excellent when material nonlinearity is included in the analysis. In this paper, a brief review of GMC is provided, along with a description of the nonlinear behavior of the constituents and associated constituent constitutive relations, and the improved macro (or composite) behavior predictions are documented and illustrated.				
14. SUBJECT TERMS Micromechanics; Composites; Elasticity; Analysts			15. NUMBER OF PAGES 31	
			16. PRICE CODE A03	
17. SECURITY CLASSIFICATION OF REPORT Unclassified	18. SECURITY CLASSIFICATION OF THIS PAGE Unclassified	19. SECURITY CLASSIFICATION OF ABSTRACT Unclassified	20. LIMITATION OF ABSTRACT	